Hindawi Publishing Corporation
International Journal of Photoenergy
Volume 2016, Article ID 9727895, 9 pages
http://dx.doi.org/10.1155/2016/9727895

Research Article

Solar Thermochemical Hydrogen Production via Terbium Oxide Based Redox Reactions

Rahul Bhosale, Anand Kumar, and Fares AlMomani

Department of Chemical Engineering, College of Engineering, Qatar University, P.O. Box 2713, Doha, Qatar

Correspondence should be addressed to Rahul Bhosale; rahul.bhosale@qu.edu.qa

Received 24 November 2015; Revised 16 December 2015; Accepted 5 January 2016

Academic Editor: Juan M. Coronado

The computational thermodynamic modeling of the terbium oxide based two-step solar thermochemical water splitting (Tb-WS) cycle is reported. The 1st step of the Tb-WS cycle involves thermal reduction of TbO_2 into Tb and O_2, whereas the 2nd step corresponds to the production of H_2 through Tb oxidation by water splitting reaction. Equilibrium compositions associated with the thermal reduction and water splitting steps were determined via HSC simulations. Influence of oxygen partial pressure in the inert gas on thermal reduction of TbO_2 and effect of water splitting temperature (T_L) on Gibbs free energy related to the H_2 production step were examined in detail. The cycle (η_{cycle}) and solar-to-fuel energy conversion ($\eta_{\text{solar-to-fuel}}$) efficiency of the Tb-WS cycle were determined by performing the second-law thermodynamic analysis. Results obtained indicate that η_{cycle} and $\eta_{\text{solar-to-fuel}}$ increase with the decrease in oxygen partial pressure in the inert flushing gas and thermal reduction temperature (T_H). It was also realized that the recuperation of the heat released by the water splitting reactor and quench unit further enhances the solar reactor efficiency. At $T_H = 2280$ K, by applying 60% heat recuperation, maximum η_{cycle} of 39.0% and $\eta_{\text{solar-to-fuel}}$ of 47.1% for the Tb-WS cycle can be attained.

1. Introduction

H_2 is considered as one of the most promising future energy sources as it is characterized by a very high energy density (143 MJ/kg) and environmentally clean utilization. H_2 can be produced by gasification and reforming of fossil fuels [1–3], pyrolysis and reforming of biomass [4–7], ethanol and methanol decomposition [8–11], and so forth. Literature survey indicates that, in recent years, the researchers are attracted more towards production of H_2 from water by using solar energy as the heat source.

Solar radiation is an essentially inexhaustible energy source that delivers about 100,000 TW to the earth. Harvesting the solar radiation and converting it effectively into renewable H_2 fuel from H_2O provide a promising path for a future sustainable energy economy. Solar H_2 production via metal oxide (MO) based thermochemical H_2O splitting reaction is considered as one of the capable new technologies for fulfillment of future energy requirement. In comparison to the high temperature direct thermolysis of H_2O, the MO based thermochemical cycle is advantageous as (a) this cycle needs lower temperatures as compared to thermolysis, (b) it has no explosive mixture formation as the production of H_2 and O_2 can be carried out in two different steps, and (c) it is environmentally and thermodynamically more feasible compared to thermolysis.

Production of solar H_2 via MO based thermochemical reactions is a two-step process. In the first step, the MO is reduced into a lower valence MO or metal with the help of solar energy. The reduced MO is further reoxidized in the second step via H_2O splitting reaction. Several MO based redox systems were theoretically and experimentally studied towards thermochemical water splitting reaction which includes ZnO/Zn cycle [12–15], Fe_3O_4/FeO cycle [16–20], SnO_2/SnO cycle [21–23], ferrite cycle [24–30], ceria cycle [31–36], and perovskite cycle [37–41]. Previous investigations indicate that these cycles are promising towards solar water splitting reaction but possess certain imitations also. The ZnO/Zn and SnO_2/SnO cycles are volatile in nature and hence material loss during multiple cycles is inevitable. On the other hand, Fe_3O_4/FeO, ferrite, ceria, and perovskite cycles depend upon the nonstoichiometry of the redox materials and hence the complete reduction and oxidation were not observed which resulted in the fact that smaller amounts of H_2 production were observed. Due to these reasons, investigations are underway to explore new thermochemical cycles for the production of H_2 via water splitting reaction.

In this study, computational thermodynamic modeling of a new terbium oxide based two-step solar thermochemical water splitting (Tb-WS) cycle was performed to determine its thermodynamic efficiency by using HSC Chemistry software and databases (HSC 7.1). Thermodynamic equilibrium composition of the solar thermal reduction of terbium oxide (step 1) and water splitting reaction (step 2) were determined. Effect of oxygen partial pressure in the inert flushing gas used inside the solar reactor during thermal reduction step on thermodynamic efficiency of the process was explored in detail. Furthermore, the effect of water splitting temperature (T_L) on Gibbs free energy associated with the oxidation of Tb (via water splitting reaction) was also explored. In addition to the thermodynamic equilibrium analysis, the solar reactor thermodynamic modeling was also carried out. Absorption efficiency of the solar reactor, solar energy input required to run the Tb-WS cycle, heat losses due to radiation, rate of heat rejected by the quench unit and water splitting reactor, Tb-WS cycle efficiency, and solar-to-fuel energy conversion efficiency were estimated. Typical redox reactions involved in the Tb-WS cycle are presented in Figure 1.

The redox reactions involved in the Tb-WS cycle are as follows:

$$TbO_2 \longrightarrow Tb\,(g) + O_2\,(g) \quad (1)$$

$$Tb + 2H_2O\,(g) \longrightarrow TbO_2 + 2H_2\,(g) \quad (2)$$

Thermodynamic data associated with TbO_2, Tb, O_2, H_2O, and H_2 as the reactive species were taken from HSC and the analysis was performed by assuming continuous operation of the solar reactor with inlet molar flow rate of TbO_2 equal to 1 mol/sec. The boiling and fusion points for Tb are 1629 and 3396 K, respectively. Similar to other lanthanides, Tb possesses low toxicity. According to Patnaik [42], the crust global abundance of Tb is estimated to be 1.2 mg/kg.

2. Equilibrium Thermodynamic Analysis

Previous investigations associated with the production of solar fuels via MO based thermochemical reactions indicate that the heat energy that is thermal reduction temperature (T_H) required to achieve complete reduction of MOs can be decreased if ultra-high purity inert flushing gas with lower oxygen partial pressures in the range of 10^{-3} to 10^{-8} atm is used during the reduction step inside the solar reactor [43, 44]. The effect of oxygen partial pressure in the inert flushing gas on thermal reduction of TbO_2 was examined in this study and the results are reported in Figure 2. The reported findings indicate that, similar to the previous MO cycles, T_H required for the thermal reduction of TbO_2 can be lowered due to the drop in the oxygen partial pressure in the inert flushing gas. For example, at oxygen partial pressure of

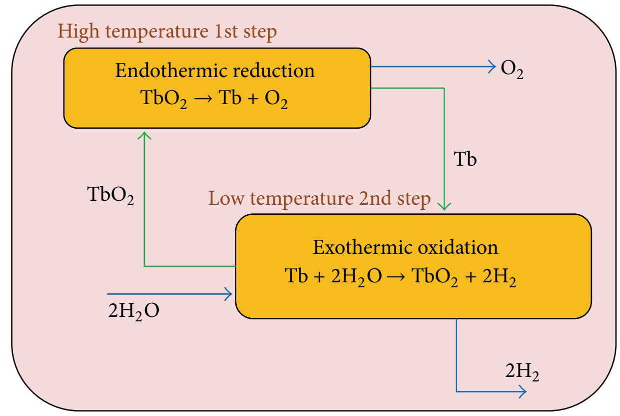

Figure 1: Typical redox reactions involved in the Tb-WS cycle.

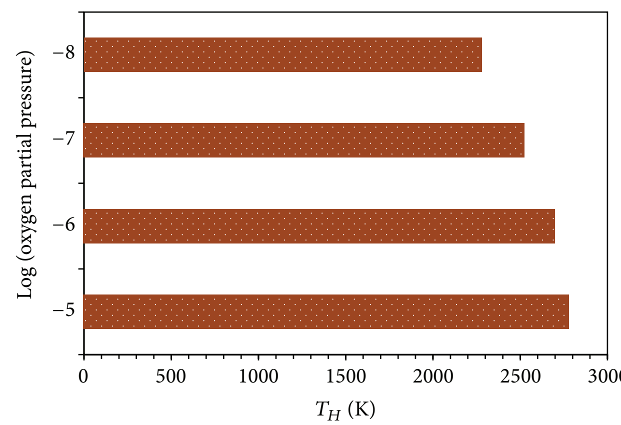

Figure 2: Influence of oxygen partial pressure in the inert flushing gas on T_H for Tb-WS cycle.

10^{-5} atm, T_H required for the complete dissociation of TbO_2 is equal to 2780 K. T_H can be decreased by 80, 260, and 500 K if the oxygen partial pressure in the inert flushing gas is reduced to 10^{-6}, 10^{-7}, and 10^{-8} atm, respectively.

In addition to T_H, the effect of oxygen partial pressure in the inert flushing gas on equilibrium compositions associated with the thermal reduction of TbO_2 was also investigated. HSC simulations reported in Figure 3 indicate that the slope of the decrease in the equilibrium concentration of TbO_2 and increase in the equilibrium concentration of Tb(g) is shifted significantly towards the lower T_H due to the decrease in the oxygen partial pressure in the inert flushing gas. The possible reason behind this shift is the reduction in the entropy of the product gases due to the drop in the oxygen partial pressure in the inert flushing gas used inside the solar reactor.

As per the HSC simulations, formation of Tb_2O_3 is an intermediate step in the thermal reduction of TbO_2 into Tb(g) and O_2(g). In addition, it was observed that the Tb formation is achieved only after decomposition of Tb_2O_3. Hence, as we are dealing with the final products, there is no need to consider Tb_2O_3 in the thermodynamic analysis. Therefore, Tb_2O_3 is not included in this study.

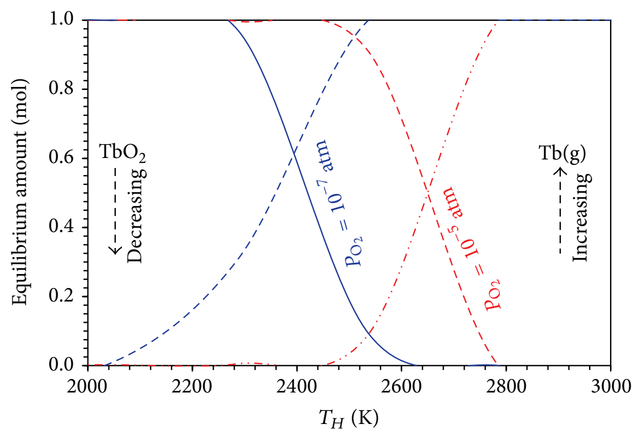

FIGURE 3: Influence of oxygen partial pressure in the inert flushing gas on equilibrium compositions associated with the thermal reduction of TbO_2.

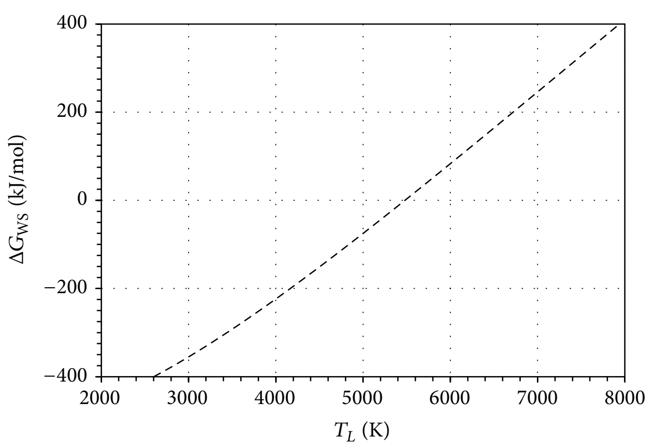

FIGURE 4: Variation in Gibbs free energy as a function of T_L for Tb-WS cycle.

Figure 4 shows the variation in the Gibbs free energy related to the water splitting reaction as a function of T_L. The Gibbs free energy change plot indicates that the hydrogen production via water splitting reaction and oxidation of Tb is feasible below 5400 K (pressure = 1 atm). It was also observed that ΔG_{WS} decreases by 434.5 kJ/mol due to the drop in T_L from 5400 to 300 K.

3. Tb-WS Solar Reactor Thermodynamic Modeling

Solar reactor operating the Tb-WS cycle was thermodynamically modeled by using the principles of the second law of thermodynamics. Figure 5 shows the process flow configuration of the Tb-WS cycle which includes a solar reactor, a quench unit, a water splitter, and an ideal H_2/O_2 fuel cell. Like the previous studies, for the solar reactor thermodynamic modeling, several assumptions were made such as the following [20]:

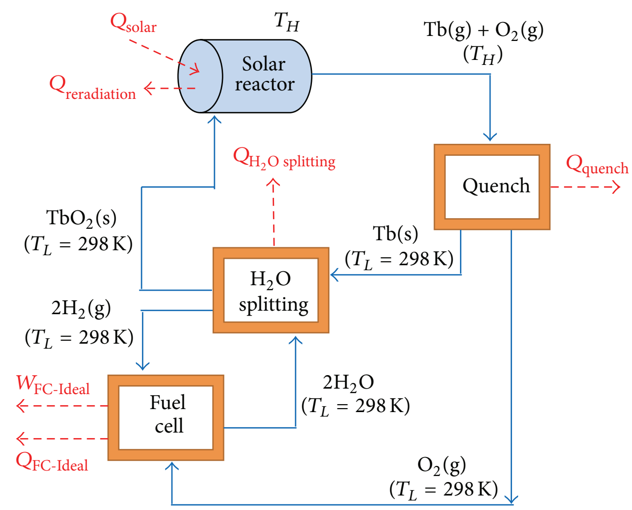

FIGURE 5: Process flow diagram for H_2 production via Tb-WS cycle.

(a) The Tb-WS solar reactor considered as a perfectly insulated blackbody absorber with effective emissivity and absorptivity equal to 1 and negligible conductive convective heat losses.

(b) Atmospheric H_2 production and steady state conditions with negligible viscous losses and kinetics/potential energies.

(c) Complete conversion of all the reactions associated with the Tb-WS cycle.

(d) Products separating naturally without laying out any work.

(e) Omission of heat exchanger required for recovering the sensible latent heat from the thermodynamic modeling.

Previously reported methodology was employed to perform the solar reactor modeling [20]. HSC Chemistry software and databases were used to get the thermodynamic properties of the reactive species and the calculations are normalized to the TbO_2 molar flow rate (1 mol/sec) entering the solar reactor.

The solar reactor absorption efficiency ($\eta_{absorption}$), which is defined as the net rate at which energy is being absorbed by the solar reactor divided by the solar energy input through the aperture, can be calculated as per

$$\eta_{absorption} = 1 - \left(\frac{\sigma T_H^4}{IC}\right), \quad (3)$$

where I is direct-normal solar irradiance (normal bean insolation) (W/m^2), C is solar flux concentration ratio (ratio of the solar flux intensity achieved after concentration to the normal beam insolation, dimensionless number) (suns), T_H is solar reactor temperature required for the thermal reduction of TbO_2 (K), and σ is Stefan-Boltzmann constant which is equal to 5.6705×10^{-8} ($W/m^2 \cdot K^4$).

Figure 6 indicates a significant improvement in $\eta_{absorption}$ due to the reduction in T_H and oxygen partial pressure in the inert flushing gas used inside the solar reactor decreases. At

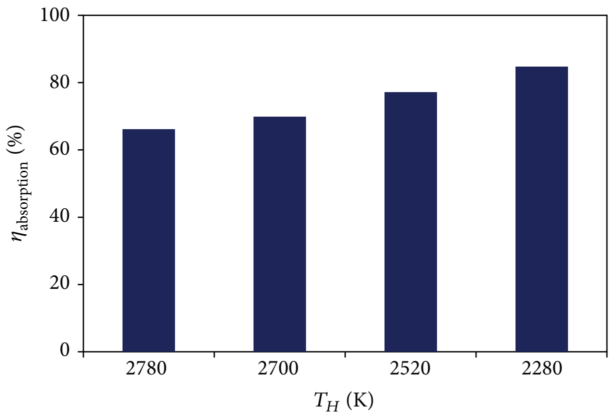

FIGURE 6: Effect of T_H on $\eta_{absorption}$.

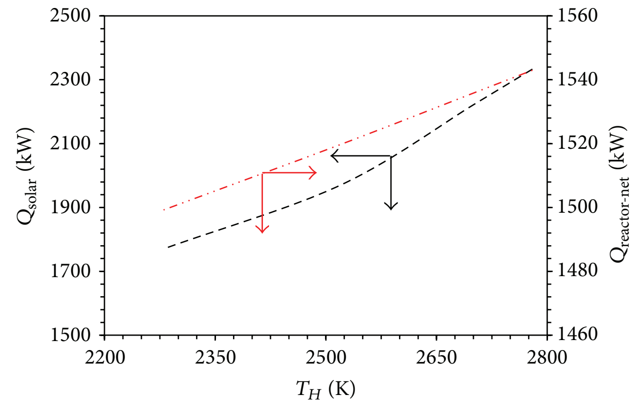

FIGURE 7: Effect of T_H on (a) Q_{solar} and (b) $Q_{reactor\text{-}net}$.

oxygen partial pressure in the inert flushing gas of 10^{-5} atm, the required T_H is 2780 K and corresponding $\eta_{absorption}$ is 66.1%. As the oxygen partial pressure in the inert flushing gas is further lowered to 10^{-7} atm, T_H can be decreased to 2520 K and $\eta_{absorption}$ can be increased up to 77.1%. As per the conditions employed in this study, the maximum $\eta_{absorption}$ that can be achieved is equal to 84.7% (oxygen partial pressure in the inert flushing gas is 10^{-8} atm and T_H is 2280 K).

In addition to the oxygen partial pressure in the inert flushing gas and T_H, C also has a significant impact on $\eta_{absorption}$. At oxygen partial pressure of 10^{-8} atm and T_H of 2280 K, the lower values of C (2000 suns) yield $\eta_{absorption}$ of 23.4%. As the value of C increases up to 3000 to 5000 suns, $\eta_{absorption}$ can get enhanced up to 48.9% and 69.3%, respectively.

The net energy required to operate the Tb-WS solar reactor can be determined according to the following equations:

$$Q_{reactor\text{-}net} = Q_{TbO_2\text{-heating}} + Q_{TbO_2\text{-reduction}} \tag{4}$$

$$Q_{TbO_2\text{-heating}} = \dot{n}\Delta H|_{TbO_2@T_L \rightarrow TbO_2@T_H} \tag{5}$$

$$Q_{TbO_2\text{-reduction}} = \dot{n}\Delta H|_{TbO_2@T_H \rightarrow Tb+O_2(g)@T_H}. \tag{6}$$

The variation in $Q_{reactor\text{-}net}$ with respect to the change in T_H is presented in Figure 7. Presented results indicate that the required $Q_{reactor\text{-}net}$ decreases with the drop in T_H and oxygen partial pressure in the inert flushing gas. As T_H is reduced from 2780 K (oxygen partial pressure in the inert flushing gas of 10^{-5} atm) to 2280 K (oxygen partial pressure in the inert flushing gas of 10^{-8} atm), $Q_{reactor\text{-}net}$ is also lowered from 1543.0 kW to 1499.2 kW, respectively.

By using the calculated $\eta_{absorption}$ and $Q_{reactor\text{-}net}$, total amount of solar energy required for the operation of the Tb-WS cycle can be estimated as

$$Q_{solar} = \frac{Q_{reactor\text{-}net}}{\eta_{absorption}}. \tag{7}$$

The decrease in Q_{solar} as a function of reduction in T_H and oxygen partial pressure in the inert flushing gas is shown in Figure 7. 2333.2 kW of solar energy is required for the operation of Tb-WS cycle when the oxygen partial pressure in the inert flushing gas is equal to 10^{-5} atm (T_H = 2780 K). Q_{solar} is reduced to 1970.3 kW as the oxygen partial pressure in the inert flushing gas is lowered to 10^{-7} atm (T_H = 2520 K). As per the modeling conditions employed in this study, the minimum Q_{solar} (1770.5 kW) is possible at oxygen partial pressure in the inert flushing gas of 10^{-8} atm (T_H = 2280 K). The reason behind this drop in Q_{solar} is the elevation in $\eta_{absorption}$ due to the fall in T_H from 2780 to 2280 K as the oxygen partial pressure in the inert flushing gas is reduced from 10^{-5} to 10^{-8} atm.

Radiation heat losses from the Tb-WS solar reactor are unavoidable as the operating temperatures are very high. These losses can be calculated as

$$Q_{reradiation} = Q_{solar} - Q_{reactor\text{-}net}. \tag{8}$$

The radiation heat losses associated with the Tb-WS cycle are presented in Figure 8(a). The plot shown indicates that, at T_H = 2780 K, 790.2 kW of heat is lost from the solar reactor due to the reradiation. However, the radiation losses are decreased due to the lowering of T_H. For instance, at T_H = 2280 K, only 271.3 kW of reradiation losses is reported as per the thermodynamic modeling. This is again due to the fact that $\eta_{absorption}$ of the Tb-WS solar reactor is higher at lower T_H.

Solar thermal reduction of TbO_2 yields Tb(g) and O_2(g). As the operating temperatures are very high, these compounds will try to recombine and reform the TbO_2. Therefore, it is highly essential to quench these compounds from T_H to T_L to avoid any recombination. During quenching, it is assumed that the chemical composition of the products remains unaltered. Due to quenching Tb(g) is cooled down to solid Tb and automatically gets separated from O_2(g). Also, during quenching, latent and sensible heat will be lost to the surroundings from the quench unit which can be estimated as

$$Q_{quench} = -\dot{n}\Delta H|_{Tb(g)+O_2(g)@T_H \rightarrow Tb(s)+O_2(g)@T_L}. \tag{9}$$

The data reported in Figure 8(b) indicates that higher amount of heat is lost due to quenching (571.4 kW) when T_H is 2780 K (oxygen partial pressure in the inert flushing gas is 10^{-5} atm).

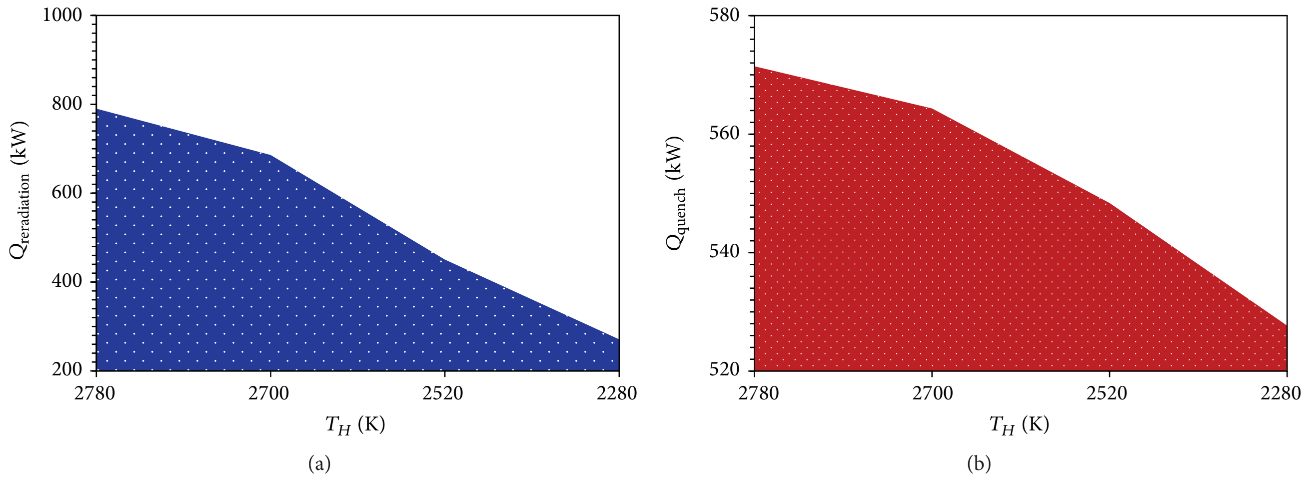

Figure 8: Effect of T_H on (a) $Q_{\text{reradiation}}$ and (b) Q_{quench}.

However, as T_H is decreased to 2280 K due to the lowering of oxygen partial pressure in the inert flushing gas (10^{-8} atm), the heat lost is reduced by 43.8 kW.

Because of the irreversible chemical transformations and reradiation losses, the irreversibilities generated in the solar reactor and the quench unit can be determined as

$$\mathrm{Irr}_{\text{reactor}} = \left(\frac{-Q_{\text{solar}}}{T_H}\right) + \left(\frac{Q_{\text{reradiation}}}{298}\right) + \dot{n}\Delta S|_{\mathrm{TbO_2}@T_L \rightarrow \mathrm{Tb(g)}+\mathrm{O_2(g)}@T_H} \quad (10)$$

$$\mathrm{Irr}_{\text{quench}} = \left(\frac{Q_{\text{quench}}}{298}\right) + \dot{n}\Delta S|_{\mathrm{Tb(g)}+\mathrm{O_2(g)}@T_H \rightarrow \mathrm{Tb(s)}+\mathrm{O_2(g)}@T_L}. \quad (11)$$

Table 1 lists the $\mathrm{Irr}_{\text{reactor}}$ and $\mathrm{Irr}_{\text{quench}}$ values as a function of T_H. From the reported numbers, it can be seen that, in case of both the Tb-WS solar reactor and quench unit, $\mathrm{Irr}_{\text{reactor}}$ and $\mathrm{Irr}_{\text{quench}}$ values are maximum at higher T_H and decrease with the reduction in T_H. For instance, $\mathrm{Irr}_{\text{reactor}}$ and $\mathrm{Irr}_{\text{quench}}$ can be lowered by 73.8% and 7.8% due to the drop in T_H from 2780 to 2280 K.

H_2 generation via water splitting reaction can be carried out at T_L of 298 K by transferring the Tb obtained after the quench unit to the water splitting reactor. The water splitting is an exothermic reaction and hence the rate of heat rejected to the surroundings from the water splitting reactor is estimated as being equal to 399.8 kW according to

$$Q_{\text{Tb oxidation}} = -\dot{n}\Delta H|_{\mathrm{Tb}+2\mathrm{H_2O} \rightarrow \mathrm{TbO_2}+2\mathrm{H_2(g)}@T_L}. \quad (12)$$

Similarly, the irreversibility associated with the water splitting reaction is estimated (1.5 kW/K) by solving

$$\mathrm{Irr}_{\text{Sm oxidation}} = \left(\frac{Q_{\text{Sm oxidation}}}{298}\right) + \dot{n}\Delta S|_{\mathrm{Tb}+2\mathrm{H_2O} \rightarrow \mathrm{TbO_2}+2\mathrm{H_2(g)}@T_L}. \quad (13)$$

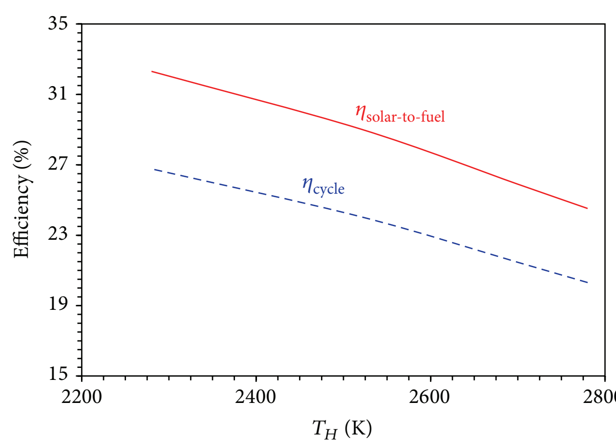

Figure 9: η_{cycle} and $\eta_{\text{solar-to-fuel}}$ as a function of T_H.

To determine the maximum work that can be extracted from the H_2 generated, an ideal H_2/O_2 fuel cell with 100% work efficiency is added to the Tb-WS cycle. According to (14) and (15), it was observed that the theoretical work performed and heat energy released by the ideal fuel cell are equal to 473.9 and 97.3 kW:

$$W_{\text{FC-Ideal}} = -\dot{n}\Delta G|_{2\mathrm{H_2(g)}+\mathrm{O_2(g)} \rightarrow 2\mathrm{H_2O(l)}@298\,\mathrm{K}} \quad (14)$$

$$Q_{\text{FC-Ideal}} = -(298)\,\dot{n}\Delta S|_{2\mathrm{H_2(g)}+\mathrm{O_2(g)} \rightarrow 2\mathrm{H_2O(l)}@298\,\mathrm{K}}. \quad (15)$$

The cycle (η_{cycle}) and solar-to-fuel conversion ($\eta_{\text{solar-to-fuel}}$) efficiency of the Tb-WS cycle can be defined as

$$\eta_{\text{cycle}} = \frac{W_{\text{FC-Ideal}}}{Q_{\text{solar}}} \quad (16)$$

$$\eta_{\text{solar-to-fuel}} = \frac{\mathrm{HHV}_{\mathrm{H_2}}}{Q_{\text{solar}}}. \quad (17)$$

Variation in η_{cycle} and $\eta_{\text{solar-to-fuel}}$ of the Tb-WS cycle as a function of T_H is presented in Figure 9. The data reported

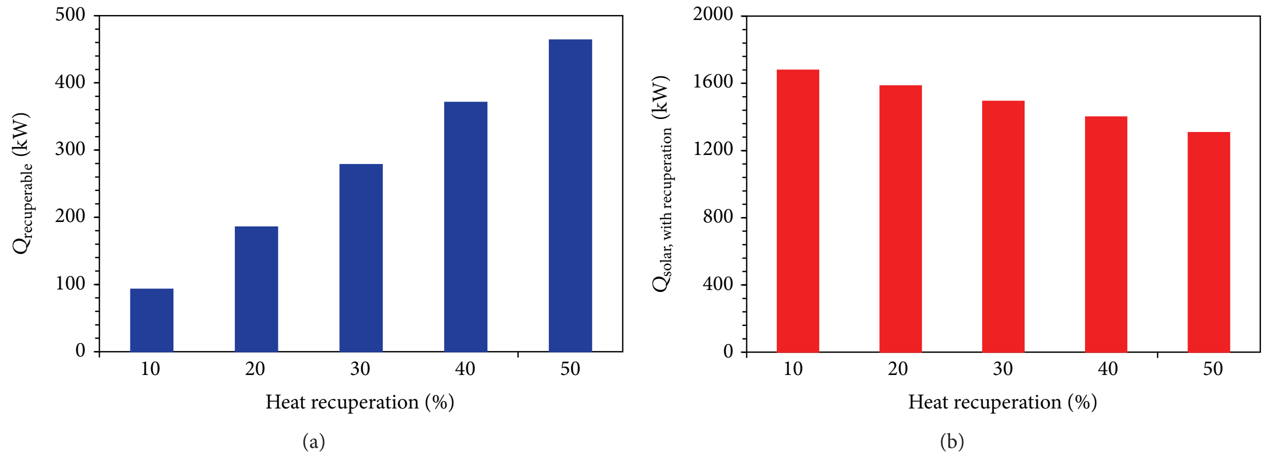

Figure 10: Effect of % heat recuperation on $Q_{solar,with\ recuperation}$ and $Q_{recuperable}$ (T_H = 2280 K).

Table 1: $Irr_{reactor}$ and Irr_{quench} as a function of T_H for Tb-WS cycle.

T_H (K)	$Irr_{reactor}$ (kW/K)	Irr_{quench} (kW/K)
2780	2.3	1.6
2700	1.9	1.6
2520	1.2	1.5
2280	0.6	1.5

indicate η_{cycle} of 20.3% and $\eta_{solar\text{-}to\text{-}fuel}$ of 24.5% at T_H of 2780 K. However, at lower T_H (2280 K), higher η_{cycle} (26.8%) and $\eta_{solar\text{-}to\text{-}fuel}$ (32.3%) can be achieved. $\eta_{solar\text{-}to\text{-}fuel}$ of the Tb-WS cycle at T_H of 2280 K is comparable to the efficiency values reported by previous investigators in case of ZnO/Zn cycle (29%), SnO_2/SnO cycle (29.8%), Fe_3O_4/FeO cycle (30%), and ceria cycle (20.2%).

η_{cycle} and $\eta_{solar\text{-}to\text{-}fuel}$ of Tb-WS cycle can be increased further by reutilizing the heat released by the water splitting reactor and quench unit. The amount of heat that can be recuperated is calculated as

$$Q_{recuperable} = Q_{quench} + Q_{Sm\ oxidation}. \tag{18}$$

As the heat released by the water splitting reactor and quench unit is recycled to run the Tb-WS cycle, the amount of solar energy required will be decreased as

$$Q_{solar,with\ recuperation} = Q_{solar} - \left[(\%\ recuperation)\, Q_{recuperable} \right]. \tag{19}$$

In case of T_H of 2280 K, Figure 10 shows that as the % heat recuperation increases, $Q_{recuperable}$ enhances whereas $Q_{solar,with\ recuperation}$ diminishes. At 10% heat recuperation, $Q_{solar,with\ recuperation}$ is equal to 1677.8 kW, which can be decreased to 1306.8 kW due to the increase in the heat recuperation up to 50%.

Table 2: η_{cycle} and $\eta_{solar\text{-}to\text{-}fuel}$ of Tb-WS cycle.

T_H (K)	η_{cycle} (%)	$\eta_{solar\text{-}to\text{-}fuel}$ (%)
Recuperation = 0%		
2780	20.3	24.5
2700	21.4	25.9
2520	24.0	29.0
2280	26.7	32.3
Recuperation = 20%		
2780	22.1	26.7
2700	23.5	28.3
2520	26.6	32.1
2280	29.9	36.0
Recuperation = 40%		
2780	24.3	29.4
2700	26.0	31.4
2520	29.7	35.9
2280	33.8	40.8
Recuperation = 60%		
2780	27.0	32.6
2700	29.1	35.1
2520	33.8	40.8
2280	39.0	47.1

After applying the heat recuperation, η_{cycle} and $\eta_{solar\text{-}to\text{-}fuel}$ associated with the Tb-WS cycle can be calculated as

$$\eta_{cycle} = \frac{W_{FC\text{-}Ideal}}{Q_{solar,with\ recuperation}}, \tag{20}$$

$$\eta_{solar\text{-}to\text{-}fuel} = \frac{HHV_{H_2}}{Q_{solar,with\ recuperation}}. \tag{21}$$

Table 2 reports η_{cycle} and $\eta_{solar\text{-}to\text{-}fuel}$ of Tb-WS cycle for different T_H and by applying 10 to 50% heat recuperation. For the data listed, it can be seen that, due to the inclusion of heat recuperation, both η_{cycle} and $\eta_{solar\text{-}to\text{-}fuel}$ of Tb-WS cycle are significantly improved. For instance, by applying

20% heat recuperation at T_H of 2280 K, η_{cycle} and $\eta_{\text{solar-to-fuel}}$ can be increased up to 23.5 and 28.4%. Likewise, at heat recuperation of 60% and T_H of 2280 K, η_{cycle} and $\eta_{\text{solar-to-fuel}}$ can get enhanced up to 39.0 and 47.1%.

According to the previous studies, the heat recuperation is highly essential to achieve higher efficiency values in case of metal oxide based solar thermochemical cycles [12, 14, 15, 17, 18, 43, 44]. In the past, attempts were made to achieve the heat recuperation in a real-life solar reactor system. For instance, Diver et al. [45] developed a heat recovery system for iron oxide cycle by using a stack of counter-rotating rings with the reactive material along the perimeter of each ring. In this system, the reactive surfaces act as extended heat transfer surfaces to achieve heat recuperation. Similarly, in case of Tb-WS cycle, heat exchangers can be coupled with the quench unit and water splitting reactor to recover the latent and sensible heat rejected by these units. Suitable heat exchanger fluid needs to be selected and the heat rejected by quench unit (due to the cooling of the thermal reduction products) and water splitting reactor (due to the exothermic splitting of water) can be stored in this fluid. This fluid can be recirculated throughout the process configuration shown in Figure 5 and the captured heat can be reutilized to run the Tb-WS cycle.

The solar reactor thermodynamic modeling performed in this paper is also verified by performing an energy balance and by evaluating the maximum achievable efficiency from the total available work and from the total solar power input. The energy balance performed in case of Tb-WS cycle (for all T_H) confirms that

$$W_{\text{FC-Ideal}} = Q_{\text{solar}} - \left(Q_{\text{reradiation}} + Q_{\text{quench}} + Q_{\text{Sm oxidation}} + Q_{\text{FC-Ideal}}\right). \tag{22}$$

As an example, at T_H of 2280 K, (22) indicates $W_{\text{FC-Ideal}}$ of 473.9 kW which is equal to $W_{\text{FC-Ideal}}$ determined by (14). Furthermore, the maximum cycle efficiency is also calculated according to

$$\eta_{\text{cycle,maximum}} = \frac{W_{\text{FC-Ideal}} + T_L\left(\text{Irr}_{\text{reactor}} + \text{Irr}_{\text{quench}} + \text{Irr}_{\text{Sm oxidation}}\right)}{Q_{\text{solar}}}. \tag{23}$$

For all T_H, it was observed that $\eta_{\text{cycle,maximum}}$ is equal to the Carnot heat engine operating between hot and cold temperature reservoirs:

$$\eta_{\text{cycle,maximum}} = 1 - \frac{T_L}{T_H} = \eta_{\text{carnot}}. \tag{24}$$

For instance, at T_H of 2280 K and T_L of 298 K, $\eta_{\text{cycle,maximum}}$ is 86.9% which is equal to $\eta_{\text{carnot}} = 86.9\%$.

4. Summary and Conclusions

Solar reactor efficiency analysis of the Tb-WS cycle for the production of H_2 via water splitting reaction was conducted by using HSC Chemistry software and databases. Simulation results indicate that the heat energy required for the complete reduction of TbO_2 into Tb and O_2 can be reduced significantly from 2780 to 2280 K by decreasing the oxygen partial pressure in the inert flushing gas from 10^{-5} to 10^{-8} atm. According to the simulations, the water splitting reaction via Tb oxidation is feasible below 5400 K.

Exergy analysis shows that $\eta_{\text{absorption}}$ of the Tb-WS solar reactor can be increased by a factor of 1.28 due to the decrease in T_H from 2780 to 2280 K. It was also observed that $Q_{\text{reactor-net}}$ and Q_{solar} can be reduced by 43.8 and 562.7 kW with the lowering of T_H from 2780 to 2280 K. Similarly, due to the similar fall in T_H, the quenching and reradiation heat losses can be dropped by 7.7 and 65.7%, respectively. The reason for the lower amounts of solar energy requirement and reduction in the heat loss via quenching and reradiation is due to the fact that $\eta_{\text{absorption}}$ of the Tb-WS solar reactor improves with the decrease in T_H. η_{cycle} of 23.5% and $\eta_{\text{solar-to-fuel}}$ of 28.4% of Tb-WS cycle at T_H of 2280 K are observed to be comparable to the previously investigated MO cycles. Furthermore, η_{cycle} and $\eta_{\text{solar-to-fuel}}$ can be further increased up to 39.0% and 47.1% by recuperating 60% of the heat rejected by the quench unit and water splitting reactor.

Nomenclature

C:	Solar flux concentration ratio, suns
HHV:	Higher heating value
I:	Normal beam solar insolation, W/m^2
MO:	Metal oxide
$\dot{n}$:	Molar flow rate, mol/sec
Q_{quench}:	Heat rejected to the surrounding from quench unit, kW
$Q_{\text{FC-Ideal}}$:	Heat rejected to the surrounding from ideal fuel cell, kW
$Q_{\text{Tb oxidation}}$:	Heat rejected to the surrounding from water splitting reactor, kW
$Q_{TbO_2\text{-heating}}$:	Energy required for heating of TbO_2, kW
$Q_{TbO_2\text{-reduction}}$:	Energy required for the thermal reduction of TbO_2, kW
$Q_{\text{reactor-net}}$:	Net energy input required for the operation of Tb-WS cycle, kW
$Q_{\text{reradiation}}$:	Radiation heat loss from the solar reactor, kW
$Q_{\text{recuperable}}$:	Total amount of heat that can be recuperated, kW
Q_{solar}:	Solar energy input, kW
$Q_{\text{solar,with recuperation}}$:	Solar power input after heat recuperation, kW
T_H:	Thermal reduction temperature, K
T_L:	Water splitting temperature, K
$W_{\text{FC-Ideal}}$:	Work output of an ideal fuel cell, kW
$\eta_{\text{absorption}}$:	Solar absorption efficiency
η_{cycle}:	Cycle efficiency
$\eta_{\text{solar-to-fuel}}$:	Solar-to-fuel energy conversion efficiency
ΔG_{WS}:	Gibbs free energy change for water splitting reaction, kJ/mol
ΔH_{WS}:	Enthalpy change for water splitting reaction, kJ/mol

ΔS_{WS}: Entropy change for water splitting reaction, J/mol·K
σ: Stefan-Boltzmann constant, 5.670×10^{-8} (W/m^2·K^4)
$Irr_{reactor}$: Rate of entropy produced across solar reactor, kW/K
Irr_{quench}: Rate of entropy produced across quench unit, kW/K
$Irr_{Sm\ oxidation}$: Rate of entropy produced across water splitting reactor, kW/K.

Conflict of Interests

The authors declare that there is no conflict of interests regarding the publication of this paper.

Acknowledgment

The authors gratefully acknowledge the financial support provided by the Qatar University Internal Grant (QUUG-CENG-CHE-14/15-10).

References

[1] N. Z. Muradov, "How to produce hydrogen from fossil fuels without CO_2 emission," *International Journal of Hydrogen Energy*, vol. 18, no. 3, pp. 211–215, 1993.

[2] N. Muradov, "Hydrogen via methane decomposition: an application for decarbonization of fossil fuels," *International Journal of Hydrogen Energy*, vol. 26, no. 11, pp. 1165–1175, 2001.

[3] M. S. Herdem, S. Farhad, I. Dincer, and F. Hamdullahpur, "Thermodynamic modeling and assessment of a combined coal gasification and alkaline water electrolysis system for hydrogen production," *International Journal of Hydrogen Energy*, vol. 39, no. 7, pp. 3061–3071, 2014.

[4] R. Tungal and R. V. Shende, "Hydrothermal liquefaction of pinewood (*Pinus ponderosa*) for H_2, biocrude and bio-oil generation," *Applied Energy*, vol. 134, pp. 401–412, 2014.

[5] A. J. Byrd, S. Kumar, L. Kong, H. Ramsurn, and R. B. Gupta, "Hydrogen production from catalytic gasification of switchgrass biocrude in supercritical water," *International Journal of Hydrogen Energy*, vol. 36, no. 5, pp. 3426–3433, 2011.

[6] D. Vera, F. Jurado, K. D. Panopoulos, and P. Grammelis, "Modelling of biomass gasifier and microturbine for the olive oil industry," *International Journal of Energy Research*, vol. 36, no. 3, pp. 355–367, 2012.

[7] P. Parthasarathy and K. S. Narayanan, "Hydrogen production from steam gasification of biomass: influence of process parameters on hydrogen yield—a review," *Renewable Energy*, vol. 66, pp. 570–579, 2014.

[8] A. Ashok, A. Kumar, R. R. Bhosale, M. A. H. Saleh, and L. J. P. van den Broeke, "Cellulose assisted combustion synthesis of porous Cu–Ni nanopowders," *RSC Advances*, vol. 5, no. 36, pp. 28703–28712, 2015.

[9] A. Cross, A. Kumar, E. E. Wolf, and A. S. Mukasyan, "Combustion synthesis of a nickel supported catalyst: effect of metal distribution on the activity during ethanol decomposition," *Industrial & Engineering Chemistry Research*, vol. 51, no. 37, pp. 12004–12008, 2012.

[10] A. Kumar, A. S. Mukasyan, and E. E. Wolf, "Impregnated layer combustion synthesis method for preparation of multicomponent catalysts for the production of hydrogen from oxidative reforming of methanol," *Applied Catalysis A: General*, vol. 372, no. 2, pp. 175–183, 2010.

[11] A. Kumar, A. Cross, K. Manukyan et al., "Combustion synthesis of copper–nickel catalysts for hydrogen production from ethanol," *Chemical Engineering Journal*, vol. 278, pp. 46–54, 2015.

[12] A. Steinfeld, "Solar hydrogen production via a two-step water-splitting thermochemical cycle based on Zn/ZnO redox reactions," *International Journal of Hydrogen Energy*, vol. 27, no. 6, pp. 611–619, 2002.

[13] S. Abanades, P. Charvin, and G. Flamant, "Design and simulation of a solar chemical reactor for the thermal reduction of metal oxides: case study of zinc oxide dissociation," *Chemical Engineering Science*, vol. 62, no. 22, pp. 6323–6333, 2007.

[14] J. R. Scheffe and A. Steinfeld, "Oxygen exchange materials for solar thermochemical splitting of H_2O and CO_2: a review," *Materials Today*, vol. 17, no. 7, pp. 341–348, 2014.

[15] D. Dardor, R. R. Bhosale, S. Gharbia, A. Kumar, and F. Al Momani, "Solar carbon production via thermochemical ZnO/Zn carbon dioxide splitting cycle," *Journal of Emerging Trends in Engineering and Applied Sciences*, vol. 6, pp. 129–135, 2015.

[16] S. Abanades and H. I. Villafan-Vidales, "CO_2 and H_2O conversion to solar fuels via two-step solar thermochemical looping using iron oxide redox pair," *Chemical Engineering Journal*, vol. 175, no. 1, pp. 368–375, 2011.

[17] M. E. Gálvez, P. G. Loutzenhiser, I. Hischier, and A. Steinfeld, "CO_2 splitting via two-step solar thermochemical cycles with Zn/ZnO and FeO/Fe_3O_4 redox reactions: thermodynamic analysis," *Energy & Fuels*, vol. 22, no. 5, pp. 3544–3550, 2008.

[18] J. E. Miller, M. D. Allendorf, R. B. Diver, L. R. Evans, N. P. Siegel, and J. N. Stuecker, "Metal oxide composites and structures for ultra-high temperature solar thermochemical cycles," *Journal of Materials Science*, vol. 43, no. 14, pp. 4714–4728, 2008.

[19] M. Roeb, J.-P. Säck, P. Rietbrock et al., "Test operation of a 100 kW pilot plant for solar hydrogen production from water on a solar tower," *Solar Energy*, vol. 85, no. 4, pp. 634–644, 2011.

[20] R. R. Bhosale, A. Kumar, L. J. P. van den Broeke et al., "Solar hydrogen production via thermochemical iron oxide-iron sulfate water splitting cycle," *International Journal of Hydrogen Energy*, vol. 40, no. 4, pp. 1639–1650, 2015.

[21] S. Abanades, "CO_2 and H_2O reduction by solar thermochemical looping using SnO_2/SnO redox reactions: thermogravimetric analysis," *International Journal of Hydrogen Energy*, vol. 37, no. 10, pp. 8223–8231, 2012.

[22] P. Charvin, S. Abanades, F. Lemont, and G. Flamant, "Experimental study of SnO_2/SnO/Sn thermochemical systems for solar production of hydrogen," *AIChE Journal*, vol. 54, no. 10, pp. 2759–2767, 2008.

[23] D. Dardor, R. Bhosale, S. Gharbia, A. AlNouss, A. Kumar, and F. AlMomani, "Solar thermochemical conversion of CO_2 into C via SnO_2/SnO redox cycle: a thermodynamic study," *International Journal of Engineering Research & Applications*, vol. 5, no. 4, pp. 134–140, 2015.

[24] C. C. Agrafiotis, C. Pagkoura, A. Zygogianni, G. Karagiannakis, M. Kostoglou, and A. G. Konstandopoulos, "Hydrogen production via solar-aided water splitting thermochemical cycles: combustion synthesis and preliminary evaluation of spinel

redox-pair materials," *International Journal of Hydrogen Energy*, vol. 37, no. 11, pp. 8964–8980, 2012.

[25] R. R. Bhosale, R. Shende, and J. Puszynski, "H_2 Generation from thermochemical water-splitting using sol-gel synthesized Zn/Sn/Mn-doped Ni-ferrite," *International Review of Chemical Engineering*, vol. 2, no. 7, pp. 852–862, 2012.

[26] R. R. Bhosale, R. V. Shende, and J. A. Puszynski, "Thermochemical water-splitting for H_2 generation using sol-gel derived Mn-ferrite in a packed bed reactor," *International Journal of Hydrogen Energy*, vol. 37, no. 3, pp. 2924–2934, 2012.

[27] R. Bhosale, R. Khadka, J. Puszynski, and R. Shende, "H_2 generation from two-step thermochemical water-splitting reaction using sol-gel derived $Sn_xFe_yO_z$," *Journal of Renewable and Sustainable Energy*, vol. 3, no. 6, Article ID 063104, 2011.

[28] R. Bhosale, R. Shende, and J. Puszynski, "H_2 generation from thermochemical water splitting using sol-gel derived Ni-ferrite," *Journal of Energy and Power Engineering*, vol. 4, pp. 27–38, 2010.

[29] F. Fresno, T. Yoshida, N. Gokon, R. Fernández-Saavedra, and T. Kodama, "Comparative study of the activity of nickel ferrites for solar hydrogen production by two-step thermochemical cycles," *International Journal of Hydrogen Energy*, vol. 35, no. 16, pp. 8503–8510, 2010.

[30] M. Neises, M. Roeb, M. Schmücker, C. Sattler, and R. Pitz-Paal, "Kinetic investigations of the hydrogen production step of a thermochemical cycle using mixed iron oxides coated on ceramic substrates," *International Journal of Energy Research*, vol. 34, no. 8, pp. 651–661, 2010.

[31] S. Abanades and G. Flamant, "Thermochemical hydrogen production from a two-step solar-driven water-splitting cycle based on cerium oxides," *Solar Energy*, vol. 80, no. 12, pp. 1611–1623, 2006.

[32] P. Furler, J. R. Scheffe, and A. Steinfeld, "Syngas production by simultaneous splitting of H_2O and CO_2 via ceria redox reactions in a high-temperature solar reactor," *Energy & Environmental Science*, vol. 5, no. 3, pp. 6098–6103, 2012.

[33] P. Furler, J. Scheffe, M. Gorbar, L. Moes, U. Vogt, and A. Steinfeld, "Solar thermochemical CO_2 splitting utilizing a reticulated porous ceria redox system," *Energy & Fuels*, vol. 26, no. 11, pp. 7051–7059, 2012.

[34] P. T. Krenzke and J. H. Davidson, "On the efficiency of solar H_2 and CO production via the thermochemical cerium oxide redox cycle: the option of inert-swept reduction," *Energy & Fuels*, vol. 29, no. 2, pp. 1045–1054, 2015.

[35] A. Le Gal and S. Abanades, "Dopant incorporation in ceria for enhanced water-splitting activity during solar thermochemical hydrogen generation," *The Journal of Physical Chemistry C*, vol. 116, no. 25, pp. 13516–13523, 2012.

[36] J. R. Scheffe, R. Jacot, G. R. Patzke, and A. Steinfeld, "Synthesis, characterization, and thermochemical redox performance of Hf^{4+}, Zr^{4+}, and Sc^{3+} doped ceria for splitting CO_2," *The Journal of Physical Chemistry C*, vol. 117, no. 46, pp. 24104–24110, 2013.

[37] A. Demont and S. Abanades, "High redox activity of Sr-substituted lanthanum manganite perovskites for two-step thermochemical dissociation of CO_2," *RSC Advances*, vol. 4, no. 97, pp. 54885–54891, 2014.

[38] A. Evdou, V. Zaspalis, and L. Nalbandian, "$La_{1-x}Sr_xFeO_{3-\delta}$ perovskites as redox materials for application in a membrane reactor for simultaneous production of pure hydrogen and synthesis gas," *Fuel*, vol. 89, no. 6, pp. 1265–1273, 2010.

[39] M. E. Gálvez, R. Jacot, J. Scheffe, T. Cooper, G. Patzke, and A. Steinfeld, "Physico-chemical changes in Ca, Sr and Al-doped La-Mn-O perovskites upon thermochemical splitting of CO_2 via redox cycling," *Physical Chemistry Chemical Physics*, vol. 17, no. 9, pp. 6629–6634, 2015.

[40] A. H. McDaniel, E. C. Miller, D. Arifin et al., "Sr-and Mn-doped $LaAlO_{3-\delta}$ for solar thermochemical H_2 and CO production," *Energy & Environmental Science*, vol. 6, pp. 2424–2428, 2013.

[41] J. R. Scheffe, D. Weibel, and A. Steinfeld, "Lanthanum–strontium–manganese perovskites as redox materials for solar thermochemical splitting of H_2O and CO_2," *Energy & Fuels*, vol. 27, no. 8, pp. 4250–4257, 2013.

[42] P. Patnaik, *Handbook of Inorganic Chemical Compounds*, McGraw-Hill, 2003.

[43] J. R. Scheffe and A. Steinfeld, "Thermodynamic analysis of cerium-based oxides for solar thermochemical fuel production," *Energy & Fuels*, vol. 26, no. 3, pp. 1928–1936, 2012.

[44] R. Bader, L. J. Venstrom, J. H. Davidson, and W. Lipiński, "Thermodynamic analysis of isothermal redox cycling of ceria for solar fuel production," *Energy & Fuels*, vol. 27, no. 9, pp. 5533–5544, 2013.

[45] R. B. Diver, J. E. Miller, M. D. Allendorf, N. P. Siegel, and R. E. Hogan, "Solar thermochemical water-splitting ferrite-cycle heat engines," *Journal of Solar Energy Engineering*, vol. 130, no. 4, Article ID 041001, 2008.